Journal of Magnetic Resonance 200 (2009) 226–232

Contents lists available at ScienceDirect

Journal of Magnetic Resonance

journal homepage: www.elsevier.com/locate/jmr

Efficient heteronuclear dipolar decoupling in solid-state NMR using frequency-swept SPINAL sequences

C. Vinod Chandran, Thomas Bräuniger *

Max-Planck-Institute of Solid-State Research, Heisenbergstr. 1, 70569 Stuttgart, Germany

ARTICLE INFO

Article history:
Received 25 May 2009
Revised 1 July 2009
Available online 9 July 2009

Keywords:
Solid-state NMR
Heteronuclear spin decoupling
SW$_f$-SPINAL
SW$_f$-TPPM
Liquid crystal NMR

ABSTRACT

Aiming to improve heteronuclear spin decoupling efficiency in NMR spectroscopy of solids and liquid crystals, we have modified the original Small Phase Incremental ALteration (SPINAL) sequence by incorporating a frequency sweep into it. For the resulting sequence, termed SW$_f$-SPINAL, the decoupling performance of a large number of sweep variants was explored by both numerical simulations and NMR experiments. It is found that introducing a frequency sweep generally increases both the 'on-resonance' decoupling performance and the robustness towards parameter offsets compared to the original SPINAL sequence. This validates the concept of extending the range of efficient decoupling by introducing frequency sweeps, which was recently suggested in the context of the frequency-swept SW$_f$-TPPM method. The sequence found to be best performing among the SW$_f$-SPINAL variants consists of fully swept 16 pulse pairs and is designated SW$_f^{lin}$(32)-SPINAL-32. Its good decoupling performance for rigid spin systems is confirmed by numerical simulations and also experimentally, by evaluating the CH_2 resonance of a powder sample of L-tyrosine under MAS. For moderate MAS frequencies, the new sequence matches the decoupling achieved with SW$_f$-TPPM, and outperforms all other tested sequences, including TPPM and SPINAL-64. SW$_f^{lin}$(32)-SPINAL-32 also shows excellent decoupling characteristics for liquid crystalline systems, as exemplified by experiments on the 5CB liquid crystal.

1. Introduction

In solid-state NMR spectroscopy of rare spins such as ^{13}C, heteronuclear spin decoupling [1–3] along with magic angle spinning [4] is routinely used to improve spectral resolution in the presence of abundant spin such as ^{1}H. Spin decoupling in solid-state NMR is especially demanding because, in rigid solids, spin–spin interactions are much stronger than in solution. In the case of solids, the continuous wave (CW) method does not perform efficiently. To improve the efficiency of heteronuclear dipolar decoupling, many composite pulse sequences have been suggested [5–23].

In 1995, Bennett et al. [5] proposed the Two Pulse Phase Modulation (TPPM) method, which strongly outperformed CW decoupling and subsequently became a routine method for dipolar decoupling in solids. In 2000, Fung et al. [6] introduced the Small Phase Incremental ALteration (SPINAL) sequence, which improved upon the performance of TPPM. In the area of oriented media, the application of efficient spin decoupling is especially important. Thus, NMR of liquid crystalline [24] and membrane systems [25,26] benefits from the resolution improvements that may be gained from high-performance proton decoupling. SPINAL was initially intended for liquid crystalline systems, but showed good efficiency also for rigid solid materials [6–8]. The TPPM sequence has a basic building block of two pulses with alternating phases $\tau_{(+\phi)}\tau_{(-\phi)}$, where τ is the pulse duration with a flip angle usually between 160° and 180°, and ϕ is the phase angle. The super-cycled SPINAL-64 has the form $Q\bar{Q}\bar{Q}Q\bar{Q}Q\bar{Q}$, and employs two additional phase increments (α and β), with Q having the specific structure $\tau_{(+\phi)}\tau_{(-\phi)}\tau_{(\phi+\alpha)}\tau_{(-\phi-\alpha)}\tau_{(\phi+\beta)}\tau_{(-\phi-\beta)}\tau_{(\phi+\alpha)}\tau_{(-\phi-\alpha)}$. For SPINAL-64, the flip angle remains similar to that of TPPM, and the most efficient phase increments usually are $\alpha = 5°$ and $\beta = 10°$. Other composite pulse sequences for decoupling include a rotor-synchronized decoupling method called X-inverse-X (XiX) [9], which has a basic unit of two 180° phase shifted pulses. XiX is known to be more efficient at high spinning speeds [9], and so is the recently suggested PISSARRO technique [10]. Recently, there has been interest in decoupling techniques working well under ultrafast MAS, and/or low RF power conditions [9–12]. In this article, we explore decoupling efficiency only for moderate spinning speeds (up to 14 kHz), where the overwhelming majority of routine measurements is still being done. Therefore, decoupling sequences specifically designed for fast and ultrafast MAS conditions, such as XiX and PISSARRO are not being considered here. In addition to the above-mentioned techniques for heteronuclear spin decoupling, a series of rotor-synchronized, symmetry-based decoupling schemes such as $C12_2^{-1}$ [13] were advanced, followed by their adiabatic versions [14]. Also, the introduction of continuous phase changes into a TPPM

* Corresponding author. Fax: +49 711 689 1502.
E-mail address: T.Braeuniger@fkf.mpg.de (T. Bräuniger).

1090-7807/$ - see front matter © 2009 Elsevier Inc. All rights reserved.
doi:10.1016/j.jmr.2009.07.006

sequence was suggested by Paëpe et al., to form a Cosine Modulated (CM) sequence [15]. An extensive theoretical analysis of decoupling sequences of the TPPM type with constant pulse durations (including CW and XiX as limiting cases for the phases angles 0° and 180°) has recently been given by Ernst and co-workers [16].

In contrast to the phase-modulated sequences with constant pulse durations [5–16], the SW$_f$-TPPM decoupling sequence [17–23] incorporates a frequency sweep (hence'SW$_f$') by using a well-defined pulse duration increment. SW$_f$-TPPM is found to outperform both TPPM and SPINAL by a small, but consistent margin, and shows improved robustness to the decoupling parameters like frequency offsets and phase angles. This was demonstrated for a variety of systems such as organic solids [17], liquid crystals [18] and inorganic solids containing quadrupolar nuclei [20]. Inside a single SW$_f$-TPPM block with N pulse pairs, the pulse duration (flip angle) of the nth pulse, τ_p^n (with $n = 0,1,\ldots,N-1$), is modified by a multiplication factor $\tau_p^n = f^n\ \tau_p$, with the duration τ_p being usually close to the value used for TPPM. The precise manner of pulse width incrementation defines a *sweep profile*. Mostly, SW$_f$-TPPM sequences with a tangential sweep profile (SW$_f^{tan}$ – TPPM, [17–20]) or linear sweep profile (SW$_f^{lin}$ – TPPM, [19,21]) have been employed. Also, sequences which simultaneously change both phase and pulse durations, SW$_{fp}$-TPPM, have newly been introduced [22,23], offering another small improvement in the decoupling efficiency.

Recently, Leskes et al. [19] attempted to quantify the benefits of introducing a frequency sweep into a decoupling sequence by using bimodal Floquet formalism [27–30]. In the resulting Hamiltonians, a residual field component along the y-direction was identified, which leads to dipolar broadening. Sequences which succeed in eliminating the I_y coefficients of the effective Hamiltonian meet the *decoupling condition* and result in efficient decoupling. For the TPPM and SPINAL sequences, the regime where the decoupling condition is met was shown to be fairly narrow. The frequency sweep performed by the SW$_f$-TPPM sequence, however, widened the region where the decoupling condition holds [19].

In the present work, we attempt to answer the question whether the decoupling performance of the SPINAL sequence may also be improved by incorporating a frequency sweep into it. To this end, we have systematically explored different sweep variants for the so-called SW$_f$-SPINAL sequence by both simulations and experiments. It is found that introducing a sweep generally improves the decoupling performance, irrespective of the sweep type, as evidenced by the experiments in a rigid organic solid system (L-tyrosine) and in a liquid crystalline system (4-*n*-pentyl-4′-cyanobiphenyl, known as 5CB). The same improvement is found by supporting numerical simulations using the SPINEVOLUTION [31] program. The best performing sequence is a swept-frequency variant of SPINAL-32, which is therefore studied in more detail.

2. Experimental

The ^{13}C Cross Polarization Magic Angle Spinning (CPMAS) spectra of natural abundance tyrosine hydrochloride (Sigma–Aldrich) were acquired on a BRUKER AVANCE-II 400 spectrometer, at a Larmor frequency of $\nu_0(^{13}C) = 100.58$ MHz, using a 4 mm MAS triple-channel probe at different spinning frequencies (8, 10, 12 and 14 kHz), with a contact time of 2 ms. Using a recycle delay of 4 s, 128 transients were accumulated for each spectrum. The ^{13}C CP experiments on the liquid crystalline system 5CB (Sigma–Aldrich) were done on the same spectrometer with a 7-mm double resonance static probe with a cross-polarization time of 5 ms. A recycle delay of 10 s was used at a temperature of 28 °C, to maintain a low duty cycle, to avoid deleterious effects on ^{13}C spectra caused by radio-frequency (RF) heating [32]. The tested decoupling sequences were implemented using the standard Bruker CPD format. The decoupling profile parameters were optimized for the different sequences, in the same way as described in previous publications [21,22]. The sweep profiles with 16 different sweep widths (and hence different slopes) were tested for both the linearly and tangentially varied SW$_f$-SPINAL sequences to find the best performance. In addition, for the tangent profiles, the tangent cut-off angle was optimized for each set of measurements, since this angle determines the curvature of the sweep profile. The tangent cut-off angle appeared to be close to 60° in most of the cases, similar to SW$_f$-TPPM [21]. In all the cases, the linear version performed as good as or sometimes even better than the tangent ones. In all the above-mentioned cases a short sweep window was favorable for the SW$_f$-SPINAL sequences.

In order to systematically verify and compare a large number of SW$_f$-SPINAL decoupling sequences, numerical simulations were done using the SPINEVOLUTION program [31]. The model spin system was a ^{13}C nucleus, dipolar-coupled with four protons arranged in a glycinyl structural backbone, and calculated with proton–proton interactions enabled. The results are displayed as the absolute intensities of the ^{13}C resonance, as a function of both the RF amplitude (ν_1) and phase angle (ϕ). Five microseconds pulse duration was chosen for all the simulations. The sequences with TPPM basic blocks were simulated at a MAS frequency of 9.0909 kHz, while the ones with SPINAL basic blocks were simulated at 8.3333 kHz MAS frequency, in order to speed up computation by avoiding interference effects with the decoupling sequence cycle. The RF amplitude ν_1 was varied from 80 to 120 kHz in step of 1 kHz while the phase angle ϕ was scanned from 5° to 35° in 1° step width. The values for the phase settings were identical for TPPM and SW$_f$-TPPM, with additional phase increments $\alpha = 5°$ and $\beta = 10°$ included for SPINAL and SW$_f$-SPINAL. A line broadening factor of 5 Hz was used for all calculations.

3. Results and discussion

3.1. Design of the SW$_f$-SPINAL pulse sequence

The first heteronuclear dipolar decoupling sequence with frequency sweep introduced was SW$_f$-TPPM [17–21], which shares its basic building block of a pulse pair with alternating phases with TPPM [5]. In most of the demonstrated cases of SW$_f$-TPPM decoupling [17–21], a sequence with 11 pulse pairs was found to have best decoupling performance. The condition for good decoupling may be achieved by adiabatic sweeps in RF field strength (ν_1) or the phase difference (2ϕ) of TPPM blocks [22]. While the SPINAL sequence exploits the modulation of phase difference of TPPM blocks, the SW$_f$-TPPM method takes advantage of sweeping the modulation frequency of the TPPM basic units, making both SPINAL and SW$_f$-TPPM less sensitive to NMR parameter changes [19]. This suggests that a combination of the phase difference modulation (as in SPINAL), with a sweep in the pulse durations (as in SW$_f$-TPPM), may be helpful to find a better decoupling sequence. To test whether a frequency sweep improves the decoupling efficiency of SPINAL, we checked several sweep variants, $\overrightarrow{Q}$, $\overrightarrow{Q\bar{Q}}$ etc., where Q is the basic SPINAL unit containing 8 pulses (i.e., $\overrightarrow{4}$ pulse pairs), and $\overrightarrow{XX\ldots}$ indicates the extension of the frequency sweep. This is schematically shown in Fig. 1. The RF sweep was implemented by multiplying the SPINAL flip angles with several incremented factors which determine a tangential or a linear sweep profile, from a smaller number less than unity to a bigger number greater than unity in a symmetrical fashion. The resulting sequence in the case of SPINAL-64 may thus have four different forms. The sequence with a RF sweep over all 64 pulses (32 pulse pairs) is represented as $\overrightarrow{Q\bar{Q}Q\bar{Q}Q\bar{Q}Q\bar{Q}}$ and is termed SW$_f$(64)-

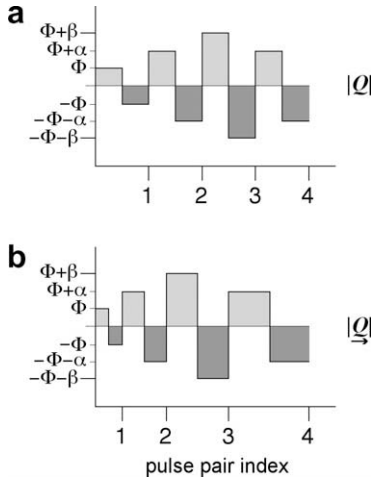

Fig. 1. Diagrammatic representation of basic building block of (a) SPINAL decoupling sequence containing four pulse pairs with the form $\tau_{(+\phi)}\tau_{(-\phi)}\tau_{(\phi+\alpha)}\tau_{(-\phi-\alpha)}\tau_{(\phi+\beta)}\tau_{(-\phi-\beta)}\tau_{(\phi+\alpha)}\tau_{(-\phi-\alpha)}$ and (b) the SW$_f$-SPINAL with an RF sweep of pulse durations τ_i.

SPINAL-64. In the same convention, SW$_f$(32)-SPINAL-64 has the form $\underrightarrow{Q\bar{Q}\bar{Q}Q}\ \underrightarrow{\bar{Q}QQ\bar{Q}}$, and the other two sweep variants are $\underrightarrow{Q\bar{Q}}\ \underrightarrow{\bar{Q}Q}\ \underrightarrow{\bar{Q}Q}\ \underrightarrow{Q\bar{Q}}$ (SW$_f$(16)-SPINAL-64) and $\underrightarrow{Q}\ \underrightarrow{\bar{Q}}\ \underrightarrow{\bar{Q}}\ \underrightarrow{Q}\ \underrightarrow{\bar{Q}}\ \underrightarrow{Q}\ \underrightarrow{Q}\ \underrightarrow{\bar{Q}}$ (SW$_f$(08)-SPINAL-64). Similarly, different block-sweep variants of SW$_f$-SPINAL-32 (16 pulse pairs) and SW$_f$-SPINAL-16 (8 pulse pairs) have been designed. For thus designed SW$_f$-SPINAL sequences, the sweep profiles were then optimised (see Experimental) and their experimental decoupling performance tested using the CH_2 resonance of L-tyrosine as a benchmark.

In Fig. 2a, the experimental decoupling efficiency of SW$_f$-SPINAL sequences with a total sequence length of 64, 32, 16 and 8 pulses and a single sweep comprising all pulses are compared for off-resonance robustness. It can be seen that the performance of all these sequences is very similar, except for the SW$_f$(32)-SPINAL-32 sequence, which shows improved characteristics. Fig. 3 shows the results from numerical simulations using the SPINEVOLUTION [31] program for the same sequences. The advantage of such simulations is that a larger parameter space of RF power and phase angle may be investigated, resulting in a somewhat more differentiated picture than that emerging from the experiments. The 2D plots in Fig. 3 show the calculated line intensities of a fictitious glycinyl structure (see Experimental), with efficient decoupling being present in the areas of high intensity. The trend that may be observed from Fig. 3 is similar to the experiments, with the SW$_f$(32)-SPINAL-32 sequence giving the best decoupling by far. In addition, we explored the effects of shortening the extent of the frequency sweeps within the SW$_f$-SPINAL-64 sequence. As can be seen from Fig. 2b, the decoupling performance deteriorates when going from SW$_f$(64)- to SW$_f$(32)-, SW$_f$(16)- and SW$_f$(08)-SPINAL-64. A similar deterioration effect was observed when shortening the sweeps within the SW$_f$-SPINAL-32 and SW$_f$-SPINAL-16 sequences.

Two significant conclusions may be derived from the data shown in Figs. 2 and 3. First, nearly all SW$_f$-SPINAL sequences perform better than the original, non-swept SPINAL-64. This clearly demonstrates that also the SPINAL sequence with its more complex phase pattern benefits from the introduction of a frequency sweep. The numerical simulation plots in Fig. 3 also show that for the swept sequences, the areas where the decoupling conditions are met are being widened. For the SW$_f$-SPINAL sequences, there is therefore a higher probability to find a combination of RF power and phase angle giving efficient decoupling than for the original SPINAL sequence. Second, we find the linearly-swept sequence with 16 pulse pairs, $\underrightarrow{Q\bar{Q}\bar{Q}Q}$ (SW$_f^{lin}$(32)-SPINAL-32), to be the best performing overall, by both experiment and numerical simulations. It may be noted that the 16 pulse pairs employed in the SW$_f^{lin}$(32)-SPINAL-32 sequence are close to the number of pulse pairs found best for SW$_f$-TPPM, creating a similar sequence cycle time τ_c. Good decoupling performance was experimentally achieved also with the $\underrightarrow{\bar{Q}QQ\bar{Q}}$ inverse sequence, even though numerical simulation results suggested that the sequence $\underrightarrow{Q\bar{Q}\bar{Q}Q}$ should be superior. In the following sections we will now evaluate the SW$_f^{lin}$(32)-SPINAL-32 sequence as the best performing of the SW$_f$-SPINAL group in more detail.

3.2. Swept-frequency SPINAL for decoupling in rigid solids

L-tyrosine hydrochloride is a suitable standard system as a rigid solid for comparative studies of the SW$_f$-SPINAL sequence, as it has been used in the demonstration of both SPINAL-64 and SW$_f$-TPPM in the original works [6,17]. The ^{13}C CPMAS signals from the aliphatic carbons of L-tyrosine (Fig. 4a), proton-decoupled with SW$_f^{lin}$(32)-SPINAL-32 method are shown in Fig. 4b, with the comparison of decoupling efficiencies being evaluated by analysis of the CH_2 resonance intensities.

Five different decoupling methods are compared in Fig. 4c and d, namely SPINAL-64, SW$_f^{lin}$(32)-SPINAL-32, SW$_f^{tan}$(32)-SPINAL-32, SW$_f^{lin}$-TPPM and SW$_f^{tan}$-TPPM, tested at four different spinning speeds. The respective parameters which determine the decoupling profiles for all different MAS frequencies used are listed in Table 1. The absolute intensities of the CH_2 resonance is plotted as a function of the decoupler frequency offset up to ±6 kHz in Fig. 4c. The expected parabolic curves [1] are reproduced for the

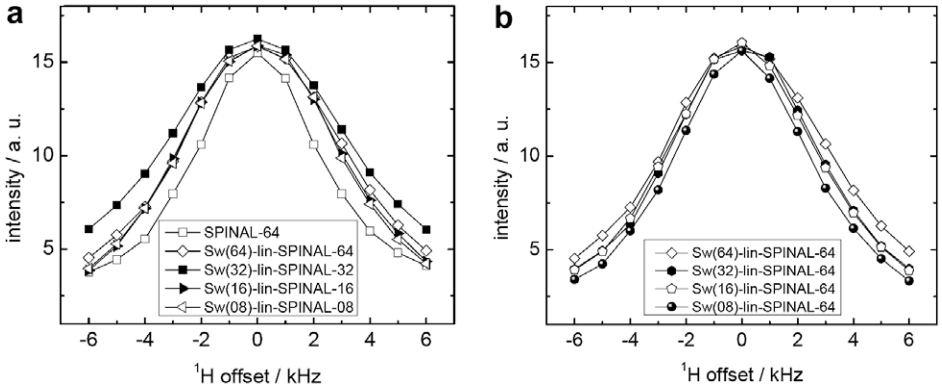

Fig. 2. ^1H off-resonance effects for the ^{13}C resonance from the methylene group of L-tyrosine hydrochloride molecule obtained with several SW$_f^{lin}$-SPINAL decoupling methods with (a) different SPINAL basic units and (b) with different SPINAL-64 sweep units obtained from its ^{13}C CPMAS spectrum at 10 kHz MAS frequency.

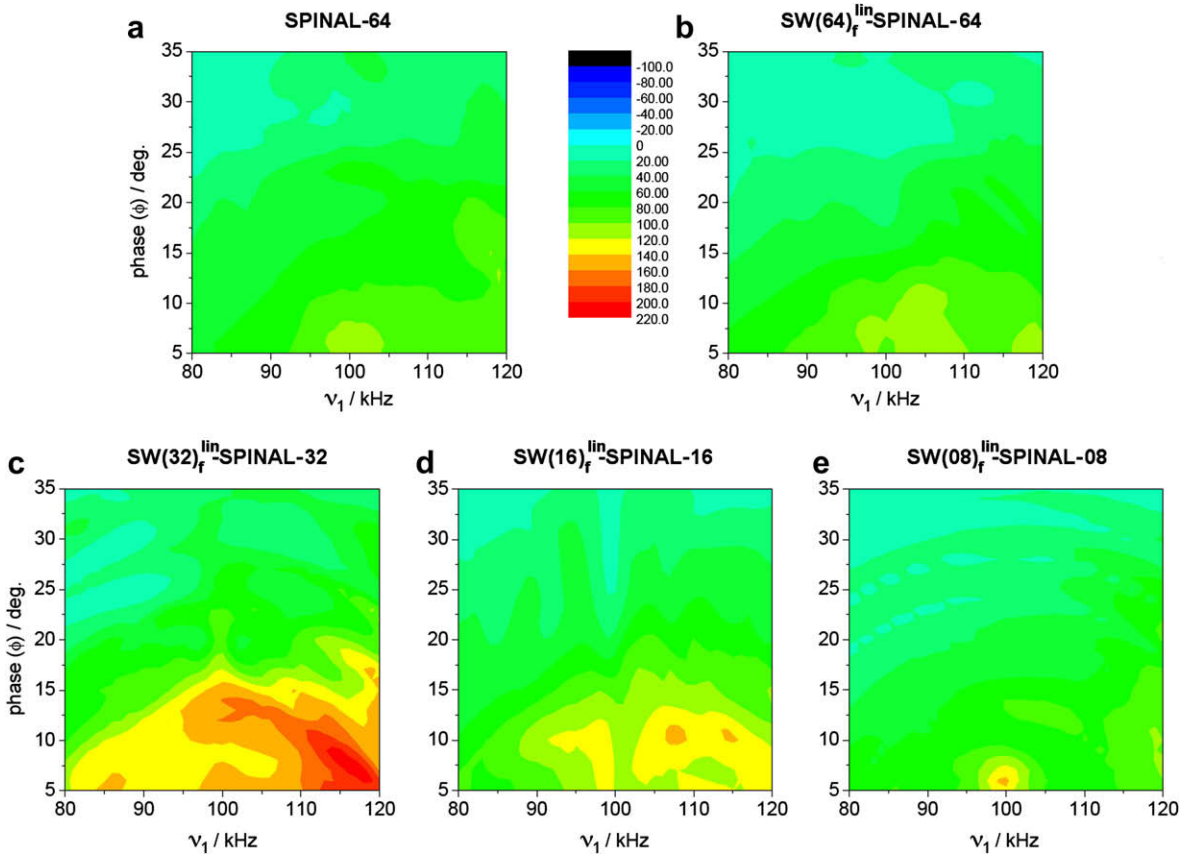

Fig. 3. The results of SPINEVOLUTION simulations [31] of (a) SPINAL-64, (b) SW$_f^{lin}$(64)-SPINAL-64, (c) SW$_f^{lin}$(32)-SPINAL-32, (d) SW$_f^{lin}$(16)-SPINAL-16 and (e) SW$_f^{lin}$(08)-SPINAL-08, being plotted as the absolute intensity of the ^{13}C resonance as a function of RF strength ν_1 and the phase angle ϕ. A four-proton system dipolar-coupled with ^{13}C was assumed for the simulations, and a MAS frequency of 8.3333 kHz was used.

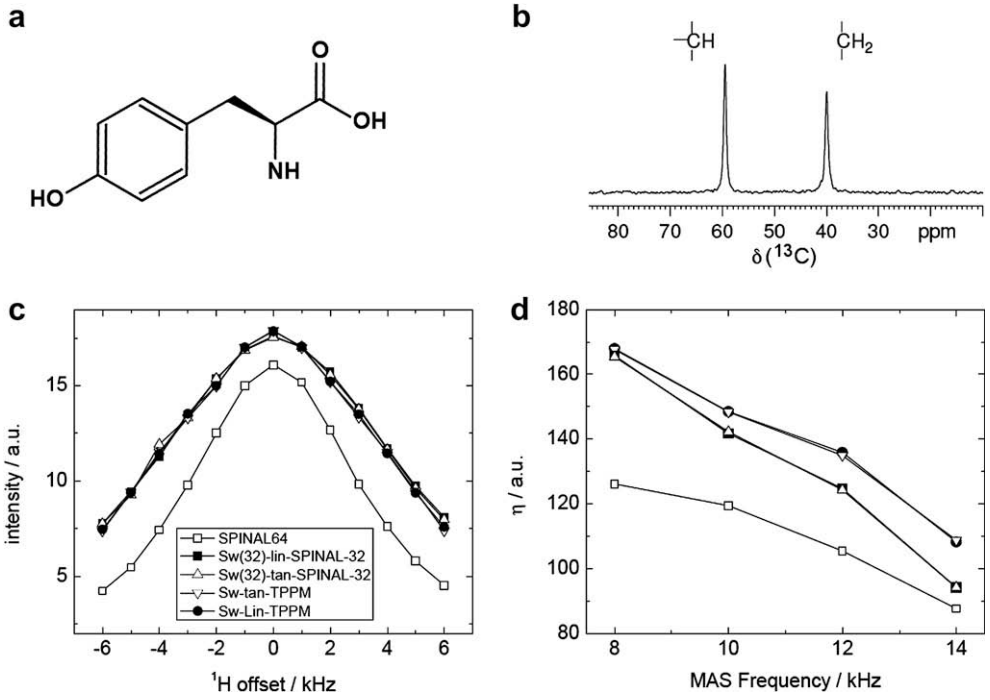

Fig. 4. (a) The L-tyrosine hydrochloride molecule and (b) its ^{13}C CPMAS spectrum of the aliphatic region. The ^{1}H off-resonance effects were studied for all the ^{13}C resonances for a range of MAS spinning frequencies and that of (c) the methylene carbon at 8 kHz MAS is shown along with (d) the MAS frequency dependence of the ^{13}C signal intensity. A figure-of-merit parameter η is introduced here [21] with $\eta = I_{0kHz} + I_{2kHz} + I_{4kHz} + I_{6kHz}$, where I_{xkHz} is the absolute intensity of the CH_2 signal at xkHz ^{1}H offset. The parameters of best-performing decoupling sequences are listed in Table 1.

Table 1
Parameters of spin decoupling sequences, optimized from ^{13}C CPMAS experiments on L-tyrosine hydrochloride. Listed are the pulse durations (τ_p), phase angle (ϕ), number of pulse pairs (N), the sweep window (W) and the tangent cut-off angle (θ). A decoupling RF field strength of 81 kHz was used in each experiment.

MAS (kHz)	Parameter	SW_f^{lin}-TPPM	SW_f^{tan}-TPPM	SW_f^{lin}-SPINAL	SW_f^{tan}-SPINAL
8	τ_p/μs	6.00	6.00	5.75	5.75
	ϕ	±7.5°	±7.5°	±6.25°	±6.25°
	N	11	11	16	16
	W	0.60–1.40	0.54–1.46	0.93–1.07	0.93–1.07
	θ	–	50°	–	50°
10	τ_p/μs	5.25	5.25	5.50	5.50
	ϕ	±7.5°	±7.5°	±6.25°	±6.25°
	N	11	11	16	16
	W	0.69–1.31	0.60–1.40	0.90–1.10	0.90–1.10
	θ	–	60°	–	60°
12	τ_p/μs	5.50	5.50	5.75	5.75
	ϕ	±7.5°	±7.5°	±6.25°	±6.25°
	N	11	11	16	16
	W	0.66–1.34	0.57–1.43	0.69–1.31	0.60—1.40
	θ	–	60°	–	55°
14	τ_p/μs	5.25	5.25	5.50	5.50
	ϕ	±7.5°	±7.5°	±6.25°	±6.25°
	N	11	11	16	16
	W	0.63–1.37	0.60–1.40	0.93–1.07	0.90–1.10
	θ	–	55°	–	65°

plots of these proton-offset dependent experiments. At 'on-resonance' conditions, the performance of SW_f-TPPM decoupling was found best, although sometimes by a very narrow margin only. The SW_f-SPINAL methods perform equally well at 8 kHz, the lowest spinning speed employed, even at zero-offset and at far-offsets, as shown in Fig. 4c. Over the entire offset range, SW_f-SPINAL was always found to be more efficient than both the original SPINAL-64 or TPPM. Both the linear and the tangent versions of SW_f-SPINAL were equally good in decoupling efficiency. However, the 'on-resonance' performance of SW_f-SPINAL drops with the increase of MAS frequency compared to SW_f-TPPM (although not beyond that of SPINAL-64), as can be seen from Fig. 4d. A robust decoupling condition is usually achieved, if the cycle time τ_c of the RF sweep is shorter than the rotor period τ_r [22]. This is what makes the SW_f-TPPM sequences with 11 pulse pairs comparably inefficient at high MAS frequencies [22]. In the case of SW_f-SPINAL, the decoupling performance falls more drastically, as the 16 pulse pairs constitute a larger τ_c than that of SW_f-TPPM. Therefore, the current versions of the SW_f-SPINAL sequence are not expected to perform well at fast and ultrafast MAS speeds. Whereas the ratio of sequence cycle time to rotor period does play a role for the obtainable decoupling efficiency, rotor-synchronisation does not appear to be of any importance for the frequency-swept sequences, in contrast to methods like XiX [9] or RS-HEPT [11].

The numerical evaluation of decoupling efficiency for the different sequences is shown in the plots of Fig. 5a–c. In the case of SW_f^{lin}-TPPM, a vertical band of high intensity which corresponds to the first occurence of the decoupling condition is clearly seen, plus periodic repeats (Fig. 5c). This band structure is similar to what has been reported before (with axes interchanged) from numerical simulations of SW_f^{tan}-TPPM decoupling with a tangent-shaped profile [19]. The periodic positions of these bands are influenced by the cycle time and the MAS frequency. In between the repeating periodic bands, there are areas of low intensity, at particular combinations of RF field strength and phase angle, which signify inefficient decoupling. In the case of SW_f-SPINAL, repeating bands are hardly visible, but a spread of moderately good decoupling condition is seen, especially in the low power region, without the appearance of the periodic troughs. As shown in Fig. 5a, the SPINAL-64 sequence is found to have a very small area of good decoupling condition in comparison with SW_f-SPINAL, which will be difficult to find by optimization. A set of simulations was also run with the MAS frequency doubled. It was found that the relative performances of the respective sequences remained unchanged, but with overall lower intensities. This corresponds to the drop in decoupling efficiency experimentally observed (Fig. 4b), as the ratio between rotor cycle τ_r and sequence cycle time τ_c becomes more unfavorable.

In summary, the advantageous effect of the frequency sweep on both decoupling efficiency and robustness of the SPINAL sequence is also clearly observed in our numerical simulations of rigid systems.

3.3. Heteronuclear dipolar decoupling in liquid crystalline systems

Highly efficient dipolar decoupling is also an important requirement in ^{13}C NMR studies of oriented media, in particular membrane [25,26] and liquid crystalline (LC) systems [24]. The demands for decoupling differ from those needed for rigid crystalline solids, as in the LC phase the dipolar interactions are scaled down by anisotropic thermal motions of the molecules. When 4-*n*-pentyl-4′-cyanobiphenyl (5CB) was initially used to demonstrate the SPINAL-64 technique [6], one of the main drawbacks shown was the severe sensitivity to the decoupler offset, especially for the aliphatic signals of the molecule [6]. In Fig. 6b, the NMR resonances from the ^{13}C spectrum of the aliphatic region of 5CB, are shown, acquired with ^{1}H decoupling using the SW_f^{lin}(32)-SPINAL-32 sequence. It can be seen clearly that all the five signals possess almost comparable intensities. This proves the high robustness of the frequency-swept SPINAL method towards ^{1}H offsets. In order to check the performance of different decoupling sequences in detail, deliberate ^{1}H offset changes were made again in the range of ±6 kHz. Different spin systems in the aliphatic region responded to it in different ways. As shown in Fig. 6c, the expected parabolic curve [1] for the offset dependence was only obtained for the most rigid α-carbon, attached to the biphenyl moiety. From the rigid part to the more mobile part, i.e., from α-carbon to the δ-carbon, there is a decrease in sensitivity towards ^{1}H offset changes, attributable to the increasing mobility of the C-atoms in the chain. Thus the

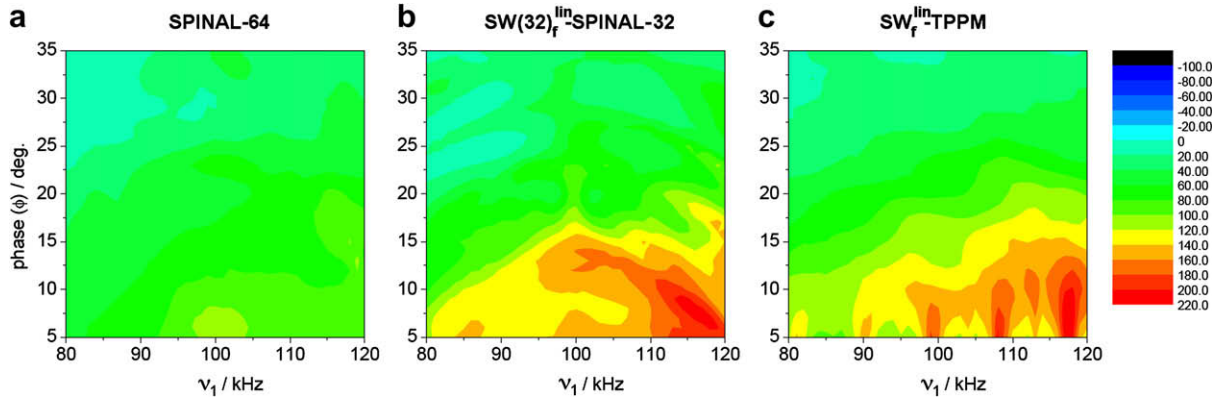

Fig. 5. The results of SPINEVOLUTION simulations [31] of (a) SPINAL-64, (b) SW$_f^{lin}$-SPINAL and (c) SW$_f^{lin}$-TPPM, being plotted as the absolute intensity of the ^{13}C resonance as a function of RF strength ν_1 and the phase angle ϕ. A four-proton system dipolar-coupled with ^{13}C was assumed for the simulations, where a MAS frequency of 8.3333 kHz was used for SPINAL-64 and SW$_f^{lin}$-SPINAL and 9.0909 kHz for SW$_f^{lin}$-TPPM.

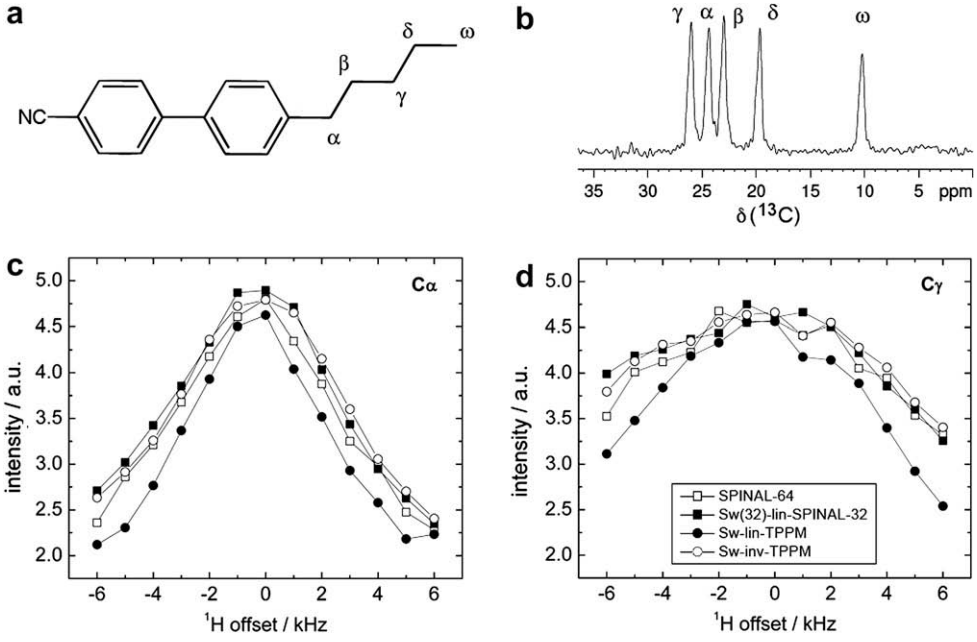

Fig. 6. (a) The 4-*n*-pentyl-4′-cyanobiphenyl (5CB) molecule and (b) its ^{13}C static CP spectrum of the aliphatic region. The ^{1}H off-resonance effects were studied for all the ^{13}C resonances and those of (c) α-carbon and (d) γ-carbon are shown. The parameters of best-performing decoupling sequences are listed in Table 2.

flattening of the offset dependence curve has its maximum with the δ-carbon, which therefore is less informative with respect to the decoupling performance, than the behavior of the signals belonging to the γ-carbon as shown in Fig. 6d. In comparison, the phenyl carbon intensities and the methyl group are not much affected with different parameter offsets and we therefore restrict the discussion to the aliphatic methylene groups.

The parameters governing different decoupling sequences had again to be optimized, before starting comparing the relative performance of them. The original TPPM sequence [5], even with the best optimized pulse duration τ_p (10.5 μs) and phase angle ϕ (7.5°) was the least efficient in decoupling and has been kept out from the comparison plots. The parameters for all decoupling methods shown in Fig. 6c and d are listed in Table 2. A low power decoupling of RF field strength of 42 kHz was used in each experiment, since RF heating of oriented samples needs to be avoided [32,33]. The sample temperature was thus held constant at 28 °C, in the nematic phase, while the crystalline phase was well below 24.0 °C and the isotropic phase existed only above 35.3 °C.

Table 2
Parameters of spin decoupling sequences, optimized from ^{13}C static CP experiments on 4-*n*-pentyl-4′-cyanobiphenyl (5CB). Listed are the pulse durations (τ_p), phase angle (ϕ), number of pulse pairs (N), and the sweep window (W). A decoupling RF field strength of 42 kHz was used in each experiment.

Parameter	SW$_f^{lin}$-TPPM	SW$_f^{inv}$-TPPM	SW$_f^{lin}$-SPINAL
τ_p/μs	11.5	11.5	11.0
ϕ	±7.5	±7.5	±12.5
N	11	11	16
W	0.81–1.19	0.67–2.00	0.90–1.10

SW$_f$-SPINAL proved to be superior to the original SPINAL-64 sequence with different 5CB aliphatic signals at 'on-resonance' and 'off-resonance' conditions, as can be seen from Fig. 6c and d. The linear as well as the tangential versions were not exactly equally efficient, the results for the linear profile being shown in the figures as it was performing slightly better. The decoupling efficiency of SW$_f$-TPPM, especially with tangent sweep profile was found to be worse than the other methods. The performance of linearly

swept SW_f-TPPM is shown in Fig. 6c and d and its comparatively low decoupling efficiency is obvious here. However, the sweep profile of SW_f-TPPM may be adapted to give better decoupling for liquid crystalline systems. It has been demonstrated by Madhu and co-workers that the so-called *inverse* sweeping profile (SW_f^{inv}-TPPM) [18] leads to efficient decoupling for the MBBA liquid crystal. Similarly here for 5CB, the SW_f^{inv}-TPPM sequence gives very good decoupling performance, of the same quality delivered by SW_f-SPINAL. Both these new sequences clearly deliver more efficient proton decoupling of liquid crystalline systems than the original SPINAL-64 sequence, especially at far offsets.

4. Conclusions

In this work, we have modified the original SPINAL sequence [6] by incorporating a frequency sweep into it, to test whether the heteronuclear decoupling performance may be further improved. This strategy is similar to that followed for frequency-swept TPPM decoupling, termed SW_f-TPPM, which was found to give excellent decoupling performance [17–23]. In analogy, the frequency-swept SPINAL variant is designated SW_f-SPINAL. For the SW_f-SPINAL sequence, we systematically explored a large number of possible sweep variants by both numerical simulations using SPINEVOLUTION [31] and NMR experiments. The NMR experiments were carried out for a rigid organic system (L-tyrosine) at a range of moderate MAS frequencies (from 8 to 14 kHz), and for a liquid crystalline system (4-*n*-pentyl-4′-cyanobiphenyl, known as 5CB). It was found that introducing a frequency sweep generally increases the decoupling efficiency, irrespective of the exact type of sweep. Also, both the 'on-resonance' decoupling performance and the robustness towards parameter offsets were found to be much improved for SW_f-SPINAL. Thus, the concept of extending the decoupling condition range by introducing frequency sweeps [19] is validated here also for the SPINAL sequence with its more complex phase pattern.

Of the numerous frequency sweep variants of SW_f-SPINAL that we tested, the sequence consisting of fully swept 16 pulse pairs (designated $SW_f^{lin}(32)$-SPINAL-32) performed best. In numerical simulations of a rigid spin system (Fig. 5), it is observed that the introduction of the frequency sweep vastly widens the area in the phase/RF-power parameter space where good decoupling is achieved in comparison to the original, non-swept SPINAL sequence. The area of good decoupling is in fact comparable to that seen for SW_f-TPPM. This excellent performance of $SW_f^{lin}(32)$-SPINAL-32 was also confirmed experimentally, by evaluating the CH_2 resonance of L-tyrosine. For the moderate MAS frequency of 8 kHz, the new sequence matches the decoupling achieved with SW_f-TPPM, and outperforms all other tested sequences. For higher spinning speeds up to 14 kHz, SW_f-SPINAL appears to be somewhat hampered by its comparatively long cycle time, with the decoupling efficiency dropping off slightly in comparison to the best performing SW_f-TPPM sequence. For liquid crystalline systems, SW_f-SPINAL shows outstanding decoupling efficiency, with robustness towards parameter offsets being improved over the original SPINAL. If high-resolution ^{13}C-NMR measurements of liquid crystalline systems are required, the $SW_f^{lin}(32)$-SPINAL-32 sequence described here, or alternatively the SW_f^{inv}-TPPM method [18], currently appear to be the best choices for achieving efficient proton decoupling.

Acknowledgment

Financial support by Deutsche Forschungsgemeinschaft (DFG Grant BR 3370/4-1) is gratefully acknowledged. The authors thank R. S. Thakur and P.K. Madhu (TIFR Mumbai) for useful discussions. We also thank K. Saalwächter (MLU Halle) for spectrometer time and support.

References

[1] D.L. VanderHart, G.C. Campbell, Off-resonance proton decoupling on-resonance and near-resonance, J. Magn. Reson. 134 (1998) 88–112.
[2] M. Ernst, Heteronuclear spin decoupling in solid-state NMR under magic-angle sample spinning, J. Magn. Reson. 162 (2003) 1–34.
[3] P. Hodgkinson, Heteronuclear decoupling in the NMR of solids, Prog. Nucl. Magn. Reson. 46 (2005) 197–222.
[4] E.R. Andrew, Magic angle spinning in solid-state NMR spectroscopy, Philos. Trans. R. Soc. Lond., Ser. A 299 (1981) 505–520.
[5] A.E. Bennett, C.M. Rienstra, M. Auger, K.V. Lakshmi, R.G. Griffin, Heteronuclear decoupling in rotating solids, J. Chem. Phys. 16 (1995) 6951–6958.
[6] B.M. Fung, A.K. Khitrin, K. Ermolaev, An improved broadband decoupling for liquid crystals and solids, J. Magn. Reson. 142 (2000) 97–101.
[7] T. Bräuniger, P. Wormald, P. Hodgkinson, Improved proton decoupling in NMR spectroscopy of crystalline solids using the SPINAL-64 sequence, Monatsh. Chem. 133 (2002) 1549–1554.
[8] G. de Paëpe, P. Hodgkinson, L. Emsley, Improved heteronuclear decoupling schemes for solid-state magic angle spinning NMR by direct spectral optimization, Chem. Phys. Lett. 376 (2003) 259–267.
[9] A. Detken, E.H. Hardy, M. Ernst, B.H. Meier, Simple and efficient decoupling in magic-angle spinning solid-state NMR: the XiX scheme, Chem. Phys. Lett. 356 (2002) 298–304.
[10] M. Weingarth, P. Tekely, G. Bodenhausen, Efficient heteronuclear decoupling by quenching rotary resonance in solid-state NMR, Chem. Phys. Lett. 466 (2008) 247–251.
[11] X. Filip, C. Tripon, C. Filip, Heteronuclear decoupling under fast MAS by a rotor-synchronized Hahn-echo pulse train, J. Magn. Reson. 176 (2005) 239–243.
[12] M. Kotecha, N.P. Wickramasinghe, Y. Ishii, Efficient low-power heteronuclear decoupling in ^{13}C high-resolution solid-state NMR under fast magic angle spinning, Magn. Reson. Chem. 45 (2007) 221–230.
[13] M. Eden, M.H. Levitt, Pulse sequence symmetries in the nuclear magnetic resonance of spinning solids: application to heteronuclear decoupling, J. Chem. Phys. 111 (1999) 1511–1519.
[14] J. Leppert, O. Ohlenschläger, M. Görlach, R. Ramachandran, Adiabatic heteronuclear decoupling in rotating solids, J. Biomol. NMR 29 (2004) 319–324.
[15] G.D. Paëpe, B. Eléna, L. Emsley, Characterization of heteronuclear decoupling through proton spin dynamics in solid-state nuclear magnetic resonance spectroscopy, J. Chem. Phys. 121 (2004) 3165–3180.
[16] I. Scholz, P. Hodgkinson, B.H. Meier, M. Ernst, Understanding two-pulse phase-modulated decoupling in solid-state NMR, J. Chem. Phys. 130 (2009) 114510.
[17] R.S. Thakur, N.D. Kurur, P.K. Madhu, Swept-frequency two-pulse phase modulation for heteronuclear dipolar decoupling in solid-state NMR, Chem. Phys. Lett. 426 (2006) 459–463.
[18] R.S. Thakur, N.D. Kurur, P.K. Madhu, Improved heteronuclear dipolar decoupling sequences for liquid-crystal NMR, J. Magn. Reson. 185 (2007) 264–269.
[19] M. Leskes, R.S. Thakur, P.K. Madhu, N.D. Kurur, S. Vega, Bimodal Floquet description of heteronuclear dipolar decoupling in solid-state nuclear magnetic resonance, J. Chem. Phys. 127 (2007) 24501.
[20] R.S. Thakur, N.D. Kurur, P.K. Madhu, An experimental study of decoupling sequences for multiple-quantum and high-resolution MAS experiments in solid-state NMR, Magn. Reson. Chem. 46 (2008) 166–169.
[21] C.V. Chandran, P.K. Madhu, N.D. Kurur, T. Bräuniger, Swept-frequency two-pulse phase modulation (SW_f-TPPM) sequences with linear sweep profile for heteronuclear decoupling in solid-state NMR, Magn. Reson. Chem. 46 (2008) 943–947.
[22] R.S. Thakur, N.D. Kurur, P.K. Madhu, An analysis of phase-modulated heteronuclear dipolar decoupling sequences in solid-state nuclear magnetic resonance, J. Magn. Reson. 193 (2008) 77–88.
[23] R.S. Thakur, N.D. Kurur, P.K. Madhu, Pulse duration and phase modulated heteronuclear dipolar decoupling schemes in solid-state NMR, in: Future Directions of Magnetic Resonance, Ind. Nat. Sci. Acad., Springer-Verlag, 2009, in press.
[24] B.M. Fung, ^{13}C NMR studies of liquid crystals, Prog. NMR. Spectrosc. 41 (2002) 171–186.
[25] S.V. Dvinskikh, K. Yamamoto, U.H.N. Dürr, A. Ramamoorthy, Sensitivity and resolution enhancement in solid-state NMR spectroscopy of bicelles, J. Magn. Reson. 184 (2007) 228–234.
[26] U.H.N. Dürr, L. Waskell, A. Ramamoorthy, The cytochromes P450 and b_5 and their reductases—promising targets for structural studies by advanced solid-state NMR spectroscopy, Biochim. Biophys. Acta 1768 (2007) 3235–3259.
[27] J.H. Shirley, Solution of the Schrödinger equation with Hamiltonian periodic in time, Phys. Rev. 138 (1965) B979–987.
[28] T.-S. Ho, S.-I. Chu, J.V. Tietz, Semiclassical many-mode Floquet theory, Chem. Phys. Lett. 96 (1983) 464–471.
[29] S. Vega, Floquet theory, in: D.M. Grant, R.K. Harris (Eds.), Encyclopedia of NMR, vol. 3, Wiley, Chichester, 1996.
[30] E. Vinogradov, P.K. Madhu, S. Vega, Strategies for high-resolution proton spectroscopy in solid-state NMR, Topics in Current Chemistry, vol. 246, Springer-Verlag, Berlin, 2005. pp. 33–90.
[31] M. Veshtort, R.G. Griffin, SPINEVOLUTION: a powerful tool for the simulation of solid and liquid state NMR experiments, J. Magn. Reson. 178 (2006) 248–282.
[32] B.M. Fung, The effect of radio-frequency heating in carbon-13 NMR studies of liquid crystals, J. Magn. Reson. 86 (1990) 160–163.
[33] D.-K. Lee, K.H. Wildman, A. Ramamoorthy, Solid-state NMR spectroscopy of aligned lipid bilayers at low temperatures, J. Am. Chem. Soc. 126 (2004) 2318–2319.